Computational Materials Science xxx (2010) xxx–xxx

Contents lists available at ScienceDirect

Computational Materials Science

journal homepage: www.elsevier.com/locate/commatsci

Damage analysis of extrusion tools made from the austenitic hot work tool steel Böhler W750

Friedrich Krumphals [a,*], Thomas Wlanis [b], Rainer Sievert [c], Volker Wieser [d], Christof Sommitsch [a]

[a] Christian Doppler Laboratory for Materials Modelling and Simulation, Institute for Materials Science and Welding, Graz University of Technology, Austria
[b] Materials Center Leoben Forschung GmbH, Leoben, Austria
[c] Bundesanstalt für Materialforschung und – prüfung, Berlin, Germany
[d] Böhler Edelstahl GmbH & Co KG, Kapfenberg, Austria

ARTICLE INFO

Article history:
Received 1 November 2009
Received in revised form 7 April 2010
Accepted 13 April 2010
Available online xxxx

Keywords:
Hot work tool steel
Damage evolution
Lifetime prediction
Copper extrusion

ABSTRACT

During hot extrusion of copper alloys, extrusion tools have to withstand cyclic thermal and mechanical loads. To enhance the service life of the tools, materials with high temperature strength are designed as well as an optimised process control is performed. To characterise the tool damage evolution during service and to improve process guiding, modelling and simulation are appropriate means. The extrusion process of copper billets at three different temperatures was simulated by an FE-program to obtain the temporal boundary conditions, i.e. stress and temperature distributions at the interface billet-liner. Those boundary conditions were used to simulate the elastic–viscoplastic behaviour of the tool steel Böhler W750 in service by means of Abaqus Standard™ v.6.8-3 software in conjunction with Z-Mat package. A lifetime rule was added in order to compute the lifetime consumption and the cycles to failure.

1. Introduction

Extrusion tools exhibit a complex strain-time pattern under a variety of cyclic loading conditions and thus are prone to failure by creep–fatigue interactions [1]. Elevated temperature failure by creep–fatigue processes is time dependent and often involves deformation path dependent interactions of cracks with grain boundary cavities. The extrusion industry tries to accelerate the manufacturing process by increasing the billet temperature and/or by accelerating the press speed that raise the loading of the tools. Additionally the tool steel producers develop enhanced more homogeneous and cleaner materials in order to increase tools lifetime. Finite element simulation of the extrusion process to get the temperature and stress evolution in the container, coupled with constitutive equations as well as lifetime consumption models in order to calculate both the inelastic strains and the tools lifetime, help to optimise the extrusion process and to compare the operating times of different hot work tool steels [2,3]. Viscoplastic constitutive models were developed in the past to take into account the inelastic behaviour of the material during creep–fatigue loads [4]. In this work, constitutive models were further developed for the austenitic hot work tool steel Böhler W750, considering the ageing of strength and materials softening at higher strain rates.

1.1. Materials

For the liner material the high temperature resistible austenitic hot work tool steel Böhler W750 (~X6NiCrTi26-15) was used, for the mantle as well as the die Böhler W300 (X38CrMoV5-1) (Table 1) and for the billet material electro copper was chosen.

2. Modelling and simulation

To predict damage, the accurate knowledge of the unsteady local thermal and mechanical loading on tools within each cycle is of particular importance. First the extrusion of a copper billet is simulated assuming rigid tools in order to obtain the time dependent temperature and radial stress boundary conditions at the inner contact area of the liner. Subsequently several extrusion cycles are simulated using an elastic–viscoplastic liner and considering the aforementioned boundary conditions.

2.1. Model for the hardening and softening behaviour

The materials model for the steel Böhler W300 can be found at Sommitsch et al. [5]. Here, this model was extended to the austenitic steel Böhler W750, which typically is used at higher temperatures.

The total strain ε of the constitutive model is decomposed into the thermal strain ε_{th}, the elastic strain ε_e, which is connected with the stress σ by Hooke's law, and into the inelastic strain ε_{in}:

* Corresponding author.
E-mail address: friedrich.krumphals@tugraz.at (F. Krumphals).

0927-0256/$ - see front matter © 2010 Elsevier B.V. All rights reserved.
doi:10.1016/j.commatsci.2010.04.022

Table 1
Chemical composition of the used tool steels in weight percent.

Grade	C	Si	Mn	Cr	Mo	Ni	V	Ti	Al	B
W300	0.38	1.10	0.40	5.0	1.30	–	0.40	–	–	–
W750	0.02	0.20	1.40	15.0	1.30	25.0	0.30	2.70	0.25	0.005

$$\boldsymbol{\varepsilon} = \boldsymbol{\varepsilon}_e(\boldsymbol{\sigma}) + \boldsymbol{\varepsilon}_{\text{in}} + \boldsymbol{\varepsilon}_{\text{th}}(T), \quad \boldsymbol{\varepsilon}_{\text{th}}(T) = \varepsilon_{\text{th}}(T)\mathbf{1} \tag{1}$$

In a viscoplastic, i.e. unified inelastic, model, creep and plasticity are covered within a single inelastic strain variable, as hardening as well as time-dependent recovery effects take place with the same dislocations, this causes the creep–plasticity interaction. According to the viscoplastic model of Lemaitre and Chaboche [6] the flow rule for the single inelastic strain $\boldsymbol{\varepsilon}_{\text{in}}$ reads:

$$\dot{\boldsymbol{\varepsilon}}_{\text{in}} = \frac{3}{2}\left\langle \frac{J_2(S-\mathbf{X}) - (k - S_{\text{el}} + \mathbf{R})}{\mathbf{K}} \right\rangle^n \frac{S-\mathbf{X}}{J_2(S-\mathbf{X})},$$
$$\langle y \rangle := \begin{cases} y, & \text{if } y > 0 \\ 0, & \text{otherwise} \end{cases} \tag{2}$$

$$S := \boldsymbol{\sigma} - \frac{1}{3}\text{tr}\boldsymbol{\sigma}\mathbf{1}, \quad J_2(\mathbf{A}) := \sqrt{\frac{3}{2}}||\mathbf{A}|| \tag{3}$$

where σ denotes the external applied stress, R the increase of the initial elastic limit k, $\mathbf{X}$ the internal back-stress, n a material parameter and S_{el} is the softening of the initial elastic limit.

The Chaboche model is based on the concept of threshold stress: if the applied stress deviator S exceeds the threshold stress (with k as the initial threshold stress), inelastic flow occurs to the extent of this overstepping.

A softening that also occurs at higher strain rates (in the range of $10^{-3}\,\text{s}^{-1}$) is likely influenced by the deformation because there would be not enough time for a solely time dependent softening. The decrease of the flow stress is predominantly related to the decrease of the elastic limit, i.e. to the lowering of the area of elastic behaviour with no plastic flow. In Eq. (4), the softening of the initial elastic limit S_{el} is introduced:

$$S_{\text{el}} = Q_{s_{\text{el}}}(T) s_{\text{el}} \tag{4}$$

with $Q_{S\text{el}}$ as the saturation parameter of the softening of k ($0 \leqslant Q_{S\text{el}} \leqslant k$) and s_{el} as the related isotropic softening variable of the elastic limit $k - S_{\text{el}} + R$,

$$\dot{s}_{\text{el}} = b_{s_{\text{el}}}(1-s)\dot{p}, \quad s_{\text{el}}(t=0) = 0, \quad \dot{p}\sqrt{\frac{3}{2}}||\dot{\varepsilon}_{\text{in}}|| \tag{5}$$

where $b_{S\text{el}}$ is a material parameter and $\dot{p}$ the von Mises equivalent inelastic strain rate.

Due to inelastic straining two kinds of hardening, denoted by the scalar R and by the tensor $\mathbf{X}$, arise. The increase R of the initial elastic limit k describes the expansion of the elastic range, the so-called isotropic hardening. As originally indicated by Olschewski et al. [7] for non-isothermal loading and discussed in [2] the following finite state function is proposed for the isotropic hardening variable, in the sense of the concept of Lemaitre and Chaboche [6] for thermo-mechanical hardening:

$$R = Q_R(T) r \tag{6}$$

with $Q_R(T)$ as the saturation parameter of R at isothermal loading, T as the temperature, and r as the related isotropic hardening variable with the evolution equation:

$$\dot{r} = b_R\left(1 - \frac{R}{Q_R}\right)\dot{p} - \frac{f}{Q_R}\left(\frac{R}{Q_R}\right)^s, \quad r(t=0) = 0 \tag{7}$$

where b_R, f and s are material parameters. b_R characterises the rate of isotropic hardening with the accumulated inelastic strain p. f and s describe the time dependent, so-called static, recovery of the deformation induced hardening: f denotes the rate of the static recovery in the fully hardened state ($R \approx Q_R$) and s the transition to the fully recovered state with time.

The parameters b_R and $b_{S\text{el}}$ as well as the saturation parameters Q_R and $Q_{S\text{el}}$ of the deformation induced softening of the viscosity describe the increase, respectively, decrease of the radius of the elastic area with preceding accumulating inelastic deformation p.

The development of the internal back-stress tensor $\mathbf{X}$ depends on the direction of deformation, i.e. it represents a strain-induced anisotropy. The evolution of $\mathbf{X}$ is related to the Bauschinger effect via the displacement of the midpoint of the elastic range, the so-called kinematic hardening (see e.g., Lemaitre and Chaboche [6]). The internal back-stress $\mathbf{X}$ is decomposed here into two parts:

$$\mathbf{X} = \mathbf{X}_1 + \mathbf{X}_2 \tag{8}$$

where $\mathbf{X}_1$ characterises the fast nonlinear kinematic hardening with inelastic strain present already at small deformation and $\mathbf{X}_2$ describes the slower hardening with inelastic strain at larger deformation ($|\varepsilon_{\text{in}}| > 0.1\,\%$). For both of them a finite state function is applied:

$$\mathbf{X}_i = \frac{2}{3}a_i(T)\boldsymbol{\alpha}_i, \quad i = 1,2 \tag{9}$$

where $a_i(T)$ are saturation parameters of the internal back-stresses $\mathbf{X}_i$ at isothermal loading and α_i are related kinematic hardening variables:

$$\alpha = c_1\phi(p)\left(\dot{\boldsymbol{\varepsilon}}_{\text{in}} - \frac{3}{2}\frac{\mathbf{X_1}}{a_1}\dot{p}\right) - \frac{3}{2}\frac{d_1}{a_1}\left(\frac{J_2(\mathbf{X}_1)}{a_1}\right)^{m_1}\frac{\mathbf{X_1}}{J_2(\mathbf{X}_1)},$$
$$\alpha_1(t=0) = 0 \tag{10a}$$

$$\phi(p) = \phi_\infty + (1-\phi_\infty)\exp(-\omega p) \tag{10b}$$

$$\alpha_2 = c_2\left(\dot{\varepsilon}_{\text{in}} - \frac{3}{2}\frac{\mathbf{X_2}}{a_2}\dot{p}\right) - \frac{3}{2}\frac{d_2}{a_2}\left(\frac{J_2(\mathbf{X}_2)}{a_2}\right)^{m_2}\frac{\mathbf{X_2}}{J_2(\mathbf{X}_2)},$$
$$\alpha_2(\mathbf{t}=0) = \mathbf{0} \tag{10c}$$

with c_i, d_i and m_i as material parameters: c_i denotes the rate of kinematic hardening with inelastic straining, d_i describes the rate of static recovery in the fully hardened state ($J_2(\mathbf{X}_i) \approx a_i$) with time and m_i the transition to the fully recovered state with time. The function $\phi(p)$ (Chaboche [8]) represents a hardening, respectively, softening of the coefficient c_1 ϕ of the kinematic hardening, where ω denotes the viscoplastic potential.

The related hardening variables r and $\boldsymbol{\alpha}_i$ describe the degree of hardening that corresponds to the accumulation of immobile dislocations in the material structure (compare, e.g., Ilschner [9]) and that causes certain internal stresses $k - S_{\text{el}} + R$ and $\mathbf{X}_i$, respectively, at a specific temperature.

Ageing of strength, i.e. a time-dependent decrease of an already initially present flow resistance at high temperatures can be described according to Lemaitre and Chaboche [6] by a time-dependent decrease of the viscosity coefficient K:

$$K = K_0(T)\kappa \tag{11}$$

with $K_0(T)$ as the initial viscosity parameter and κ as the related ageing variable with the evolution equation:

$$\dot{\kappa} = -\frac{b_k}{K_0}\langle K - K_{\infty 1}\rangle\dot{p} - \frac{g}{K_0}\left(\frac{\langle K - K_{\infty 2}\rangle}{K_0 - K_{\infty 2}}\right)^z, \quad \kappa(t=0) = 1 \tag{12}$$

where g, z, b_K, $K_{\infty 1}$ and $K_{\infty 2}$ are material parameters: g characterises the rate of ageing at the beginning of loading ($K = K_0$), z describes the transition to the fully aged material state and $K_{\infty 2}$ is the viscosity in this state. b_K and the saturation parameter $K_{\infty 1}$ of the deformation induced softening of the viscosity K describe the decrease of the viscose stress with advancing accumulating inelastic deformation p and hence partly also the drop of the extend of the stress decrease at the initial relaxation in different cycles of a reversal

strain experiment. The thermodynamic consistency of this description of ageing is given corresponding to the proof of Chaboche [10] and Cailletaud et al. [11]. The related ageing variable κ describes the degree of ageing, which can be caused, e.g., by a coarsening of second phase particles, due to a long time exposure to a high temperature.

All thermo-physical and material parameters of material Böhler W750 are temperature-dependent and have been determined for temperatures in the range of 650 °C–850 °C with 50 °C temperature steps. The values of the parameters for one temperature are given in Table 2. With respect to the calibration of the constitutive model it has to be said in particular, that strong attention must be paid to the attribution of the terms in the constitutive equations to the individual phenomena of the hardening or softening behaviour observed in the experiments in order to determine the corresponding material parameters. This procedure is outlined in [2], especially with respect to the hardening phenomena (e.g., isotropic and kinematic hardening appearing, respectively, in the diameter and the midpoint of the elastic range within the quasi-linear ranges in the hysteresis loops at unloading). For the elaboration of the determination of the material parameters of the time dependencies, i.e. primary rate dependence (n, K_0), static recovery (d_i, m_i; f, s) and ageing (g, z, K_∞), it is referred to Sommitsch et al. [5].

At 750 and 800 °C hot work steel W750 shows a decrease of the flow stress after initial hardening at a strain rate of 10^{-3} s^{-1}, see Eqs. (11) and (12) as well as Fig. 1 for 800 °C. This can be related to the kinetic of the metastable intermetallic γ′-phase. This phase transforms into the stable η-phase after longtime annealing between 750 and 850 °C. The transformation is enhanced by mechanical loading. The solid solution temperature of γ′-phase was found to be at 855 °C.

For the determination of the hardening parameters, hysteresis loops of strain-controlled cyclic tests without hold-times have been evaluated as described in [2]. Exemplarily, simulation and experiment of hysteresis loops with strain hold-time of 300s at 800 °C are shown in Fig. 2 for W750.

2.2. A lifetime model

Cyclically loaded structures suffer a fatigue failure. Fatigue lifetime means in a macroscopic model the initiation of a macro-crack (typically a fraction of millimetre). Fatigue lifetime rules are usually formulated on the basis of mean quantities of a cycle, like stress or strain ranges. In contrast, time-incremental lifetime rules evaluate the total damage in each time increment and, thus, can be applied also to complex multiaxial loading paths, for which the definition of a single loading parameter describing the entire cycle could be difficult. Furthermore, a time-incremental lifetime rule can easily be implemented in a material sub-routine for finite element analysis of structures just as an evolution equation for an additional internal variable, the lifetime consumption D, $0 \leqslant D \leqslant 1$. The following lifetime rule has been used:

$$\frac{dD}{dt} = \left(\frac{\sigma_{d\_eq}}{A}\right)^{m_l} \left(\frac{\dot{p}}{\dot{p}_0}\right)^{n_l} \dot{p}_0 \tag{13}$$

with p_0 as a normalisation constant and the material parameters A and m_l, respectively, denote the stress dependence of the lifetime behaviour. The parameter n_l describes the time-dependence of the lifetime: for rate-independent behaviour is n_l equal to 1; n_l equals zero means that a fully time-dependent lifetime behaviour is present. n_l was found to be positive but significantly lower than 1 for the investigated high temperature loading. The parameters A and m_l were determined from LCF tests with strain rates of 10^{-3} s^{-1} and without hold-times. The parameter n_l was identified by the influence of hold-times in LCF tests on the lifetime behaviour (Table 3). More details can be found at Sommitsch et al. [2].

To consider the influence of the stress triaxiality R_v, the damage equivalent stress σ_{d_eq} was used, which is a one-dimensional stress. For a certain value of the damage, the damage equivalent stress yields the same value of the elastic strain energy density as that of a three-dimensional state:

$$\sigma_{d\_eq} = \sigma_{eq}\sqrt{R_v}, \quad \sigma_{eq} := \sqrt{\frac{3}{2}\|\sigma'\|} \tag{14}$$

and

$$R_v = \frac{2}{3}(1+\nu) + 3(1-2\nu)\left(\frac{\sigma_H}{\sigma_{eq}}\right)^2 \tag{15}$$

where σ_H denotes the hydrostatic stress. The numbers of cycles to failure N_f were calculated for the seek of simplicity by,

$$N_f \approx 1/(\Delta D)_S \tag{16}$$

where $(\Delta D)_S$ is the lifetime consumption within a stabilized cycle. Both model adaptation and validation always referred to the third cycle. At the investigated high temperatures, subsequent cyclic softening appeared without any saturation of the hysteresis loops, but integration of the time-incremental lifetime rule over all cycles up to the fatigue failure ($D = 1$) would be too costly for a real component. Nevertheless, the damage rate takes into account the whole loading complexity within a cycle.

2.3. Extrusion model and FEM simulation of the copper extrusion process

To predict damage, the accurate knowledge of the unsteady local thermal and mechanical loading within one cycle onto the inner diameter of the liner is of particular importance. Hence the thermo-mechanical load of a container during extrusion of a billet was analysed with DEFORM™2D. The container assembly is symmetrical therefore a 2D axis-symmetric model of the container was used. The ram was assumed to be rigid, the die, liner and mantle were assumed to be elastic. The configuration of the extrusion model is depicted in Fig. 3.

The length L, inner diameter D_i and outer diameter D_o of the liner, mantle and billet, respectively, have been assumed to be:

Liner: $L = 115$ mm; $D_i = 45$ mm; $D_o = 105$ mm.
Mantle: $L = 115$ mm; $D_i = 105$ mm; $D_o = 270$ mm.
Billet: $L = 100$ mm; $D = 45$ mm.

The simulated extrusion process in DEFORM™2D includes the shrink-fitting of the mantle (0.8‰), the pre-heating of the container to a working temperature of 500 °C, the pressing on the container against the die and the forward extrusion of the billet with a ram speed of 7 mm/s, which causes complex load cases.

Table 2
Values of the material parameters for the elastic–viscoplastic Chaboche model determined for the hot work tool steel W750 at 700 °C.

E (MPa)	148,000	g (MPa $s^{(1-1/n)}$)	0
K_0 (MPa $s^{1/n}$)	200	z	(0.4)
n	5	a_1 (MPa)	295
k (MPa)	100	c_1	7000
Q_R (MPa)	150	ϕ_∞	0.45
b_R	2200	ω	3000
f (MPa/s)	0.5	a_2 (MPa)	200
q	4	c_2	300
Q_S (MPa)	0	d_1 (MPa/s)	13
b_S	(0)	m_1	7.8
$K_{\infty 1}$ (MPa $s^{1/n}$)	200	d_2 (MPa/s)	45
b_K	(0)	m_2	1.5
$K_{\infty 2}$ (MPa $s^{1/n}$)	(100)		

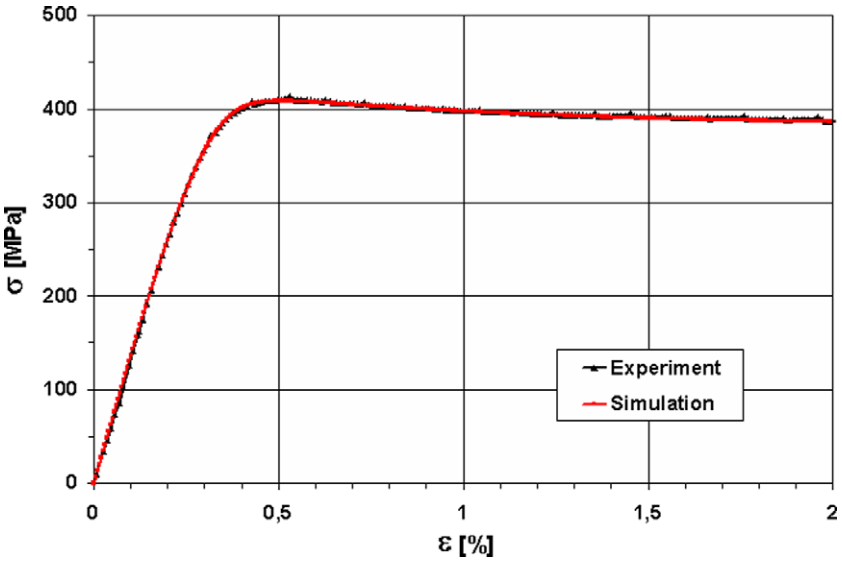

Fig. 1. Flow curve of the hot work tool steel Böhler W750 at 800 °C and a strain rate of 10^{-3} s^{-1}.

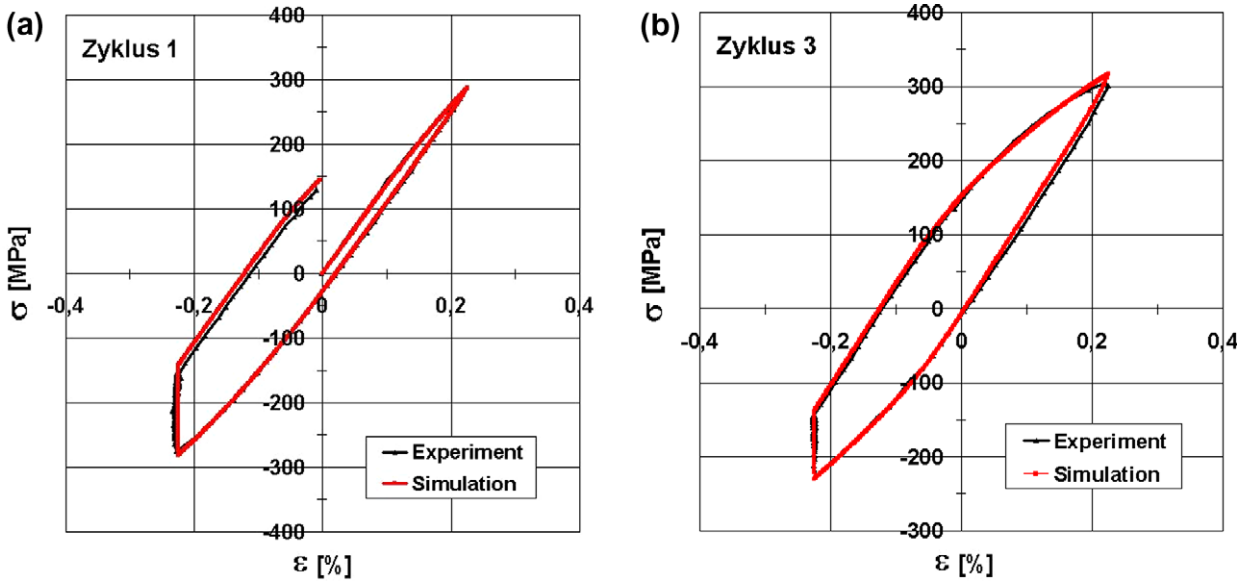

Fig. 2. Stress–strain behaviour at cyclic loading for the same temperature and strain rate as in Fig. 1 with a hold-time of 300 s after: (a) one and (b) three cycles, comparison of simulation and experiment.

Table 3
Material parameter values of the lifetime rule for the W750 hot work tool steel for the temperature of 700 °C.

m_l	6
A (MPa)	460
n_l	0.53
$\dot{p}_0$ (1/s)	10^{-4}

The temperature and pressure values according to three different process conditions, namely a varying billet temperature of 850, 900 and 950 °C, respectively, were committed as boundary conditions to ABAQUS Standard™ v.6.8-3 calculations with the elastic–viscoplastic liner and elastic mantle. The calculated boundary conditions have been compared to measured ones, which is described in detail in [12].

Fig. 4 shows a snap-shot of the accumulated viscoplastic strain as well as the temperature distribution in the container during the third extrusion cycle. The non-uniform stress distribution is a result of the complex load cases.

For the liner the constitutive model showed above was implemented explicitly by means of Z-Mat package [13]. The uncoupled lifetime consumption model was added as well.

2.4. Damage evolution and lifetime prediction

The same configuration which is depicted in Fig. 4, was used to predict the damage evolution for a selected point at the area of maximum lifetime consumption at the inner liner wall during the copper extrusion process with three different billet temperatures. The lifetime consumption of the third cycle (see ΔD in

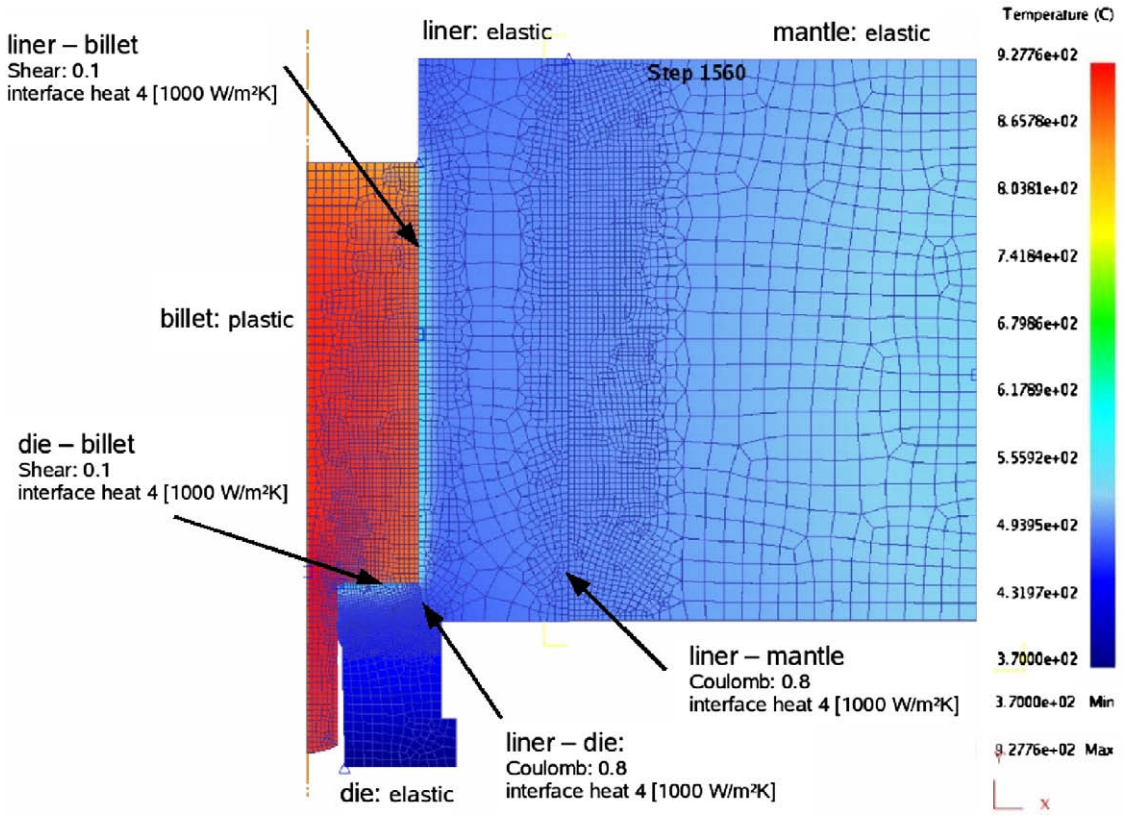

Fig. 3. Axis-symmetrical model and temperature distribution describing the extrusion of a 900 °C copper billet in DEFORM™2D with friction and heat transfer conditions (marked by arrows).

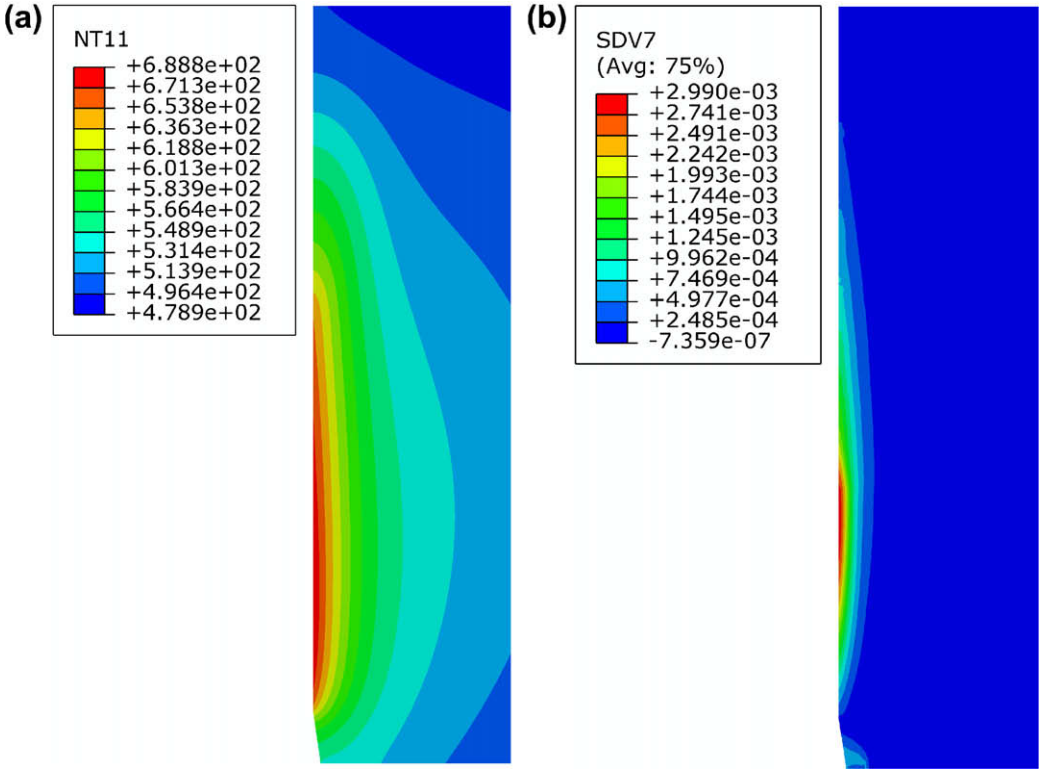

Fig. 4. (a) Temperature (°C) distribution in the liner during the third extrusion cycle and (b) accumulated inelastic strain after the third cycle with a billet temperature of 950 °C; ABAQUS Standard™ v.6.8-3.

Please cite this article in press as: F. Krumphals et al., Comput. Mater. Sci. (2010), doi:10.1016/j.commatsci.2010.04.022

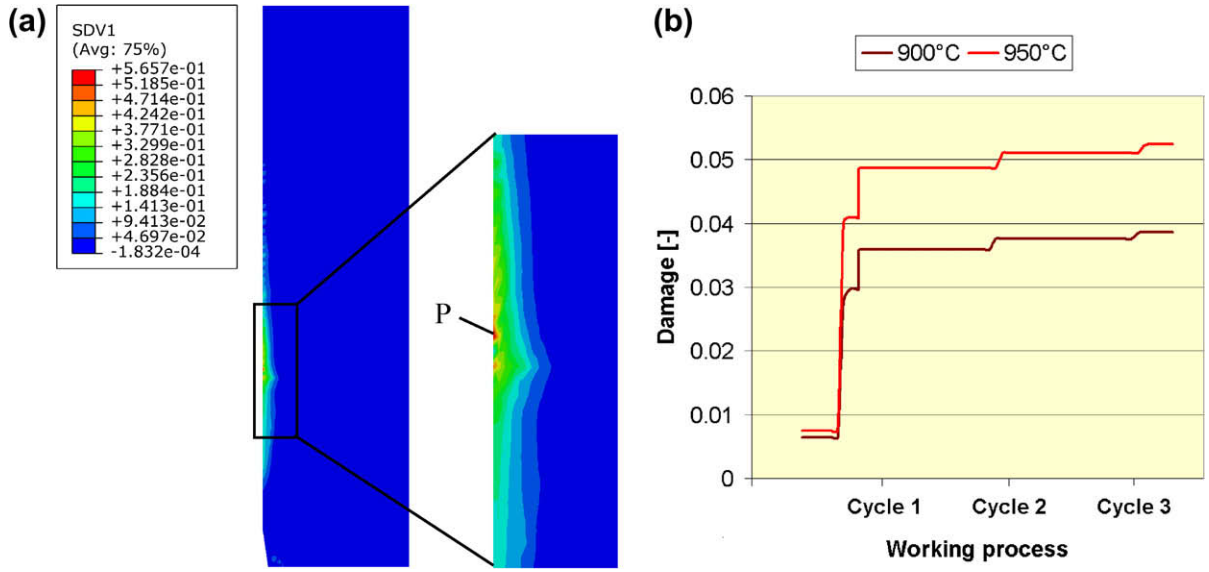

Fig. 5. (a) Resulting creep–fatigue damage according to 950 °C billet temperature as well as (b) the lifetime consumption for two different process conditions during three cycles of one point of maximum damage (*P*) at the inner wall of the liner (see Fig. 4); ABAQUS Standard™ v.6.8-3 in conjunction with Z-Mat.

Fig. 5b) was chosen representatively to calculate the lifetime to failure, which is 1050 and 750 cycles until failure occurs according to the billet temperatures of 900 and 950 °C. Fig. 5a depicts the damage distribution after the third extrusion cycle for the hot work tool steel W750. The largest accumulated damage occurs in regions that exhibit maximum accumulated inelastic strain and damage equivalent stress loading (compare Figs. 4 and 5a).

Observing the obtained results, a significant reduction of tool lifetime occurs at initial higher billet temperatures. Cyclic thermal loads close to 700 °C are shown to be critical for the tools. The highest thermo-mechanical loaded area in the liner is the lower region close to the inner surface, which stays longer in contact with the copper billet than the top region and therefore also has to bear mechanical loads for longer time intervals. Accelerating the ram speed would reduce the thermal loading, however could slightly increase mechanical loads. For hot extrusion of aluminium, the austenitic hot work tool steel W750 in general is not used because of the lower occurring temperatures. Therefore ferritic tool steels of type EN 1.2343 are suitable, which exhibits better material strength at lower temperatures.

3. Conclusions

The lifetime of a liner made of an austenitic hot work tool steel during copper extrusion was predicted. Therefore the extrusion process was simulated in order to get both temperature and radial stress boundary conditions for a subsequent cyclic simulation of the temperature and stress evolution in the container. An advanced elastic–viscoplastic constitutive model was coupled by means of Z-Mat package in Abaqus Standard and a time-incremental lifetime rule was added. It was shown that it is possible to find optimum process conditions to enhance the service life of the tool, which was found for moderate billet temperatures that neither cause extreme thermal nor mechanical loads. The critical regions of the tools are generally edges, diminutions and areas under high stress triaxialities and large accumulated inelastic strains, respectively.

Acknowledgements

The authors would like to thank very much the Federal Institute for Materials Research and Testing (BAM), Divison V.2 "Mechanical Behaviour of Materials" for performing the tests and Böhler Edelstahl GmbH as well as the Christian Doppler Research Association in Vienna for the financial support of the project.

References

[1] V. Wieser, C. Sommitsch, P. Haberfellner, H. Lehofer, New developments in the design and production of container assemblies, in: ET '04 – Proc. 8th Inter. Aluminium Extrusion Technology Seminar, Orlando, vol. 1, 2004, pp. 309–316.
[2] C. Sommitsch, T. Wlanis, T. Hatzenbichler, V. Wieser, Steel Grips 4 (2006) 51–55.
[3] C. Sommitsch, R. Sievert, T. Wlanis, C. Redl, Comput. Mater. Sci. 43 (2008) 82–91.
[4] J.-L. Chaboche, J. Appl. Mech. 60 (1993) 813–821.
[5] C. Sommitsch, R. Sievert, T. Wlanis, B. Günther, V. Wieser, J. Comput. Mater. Sci 39 (2007) 55–64.
[6] J. Lemaitre, J.-L. Chaboche, Mechanics of Solid Materials, Cambridge Univ. Press, 1990.
[7] J. Olschewski, R. Sievert, A. Bertram, et al., Aspects of high temperature deformation and fracture in crystalline materials, (JIMIS-7), in: Y. Hosoi, (Ed.), The Japan Institute of Metals, Nagoya, 1993, pp. 641–648.
[8] J.-L. Chaboche, Viscoplastic constitutive equations for the description of cyclic and anisotropic behaviour of metals, Bulletin de L'Academie Polonaise des Sciences, Serie des Sciences Techniques, vol. 25, 1977, pp. 33–41.
[9] B. Ilschner, Hochtemperatur-Plastizität, Springer Verlag, 1973.
[10] J.-L. Chaboche, Unified cyclic viscoplastic constitutive equations, in: A.S. Krausz, K. Krausz (Eds.), Development, Capabilities and Thermodynamic Framework in Unified Constitutive Laws of Plastic Deformation, Academic Press, 1996, pp. 1–68.
[11] G. Cailletaud, C. Depoid, D. Massinon, E. Nicouleau-Bourles, Elastoviscoplasticity with aging in aluminium alloys, in: G.A. Maugin et al. (Eds.), Continuum Thermomechanics, Kluwer Academic Publishers, 2000, pp. 75–86.
[12] F. Krumphals, T. Wlanis, C. Sommitsch, C. Redl, Comput. Methods Mater. Sci. 7 (2007) 47–53.
[13] Northwest Numerics and Modeling, Inc., 150 Nickerson Street, Suite 102, Seattle, WA 98109, <http://www.nwnumerics.com/Z-mat>.